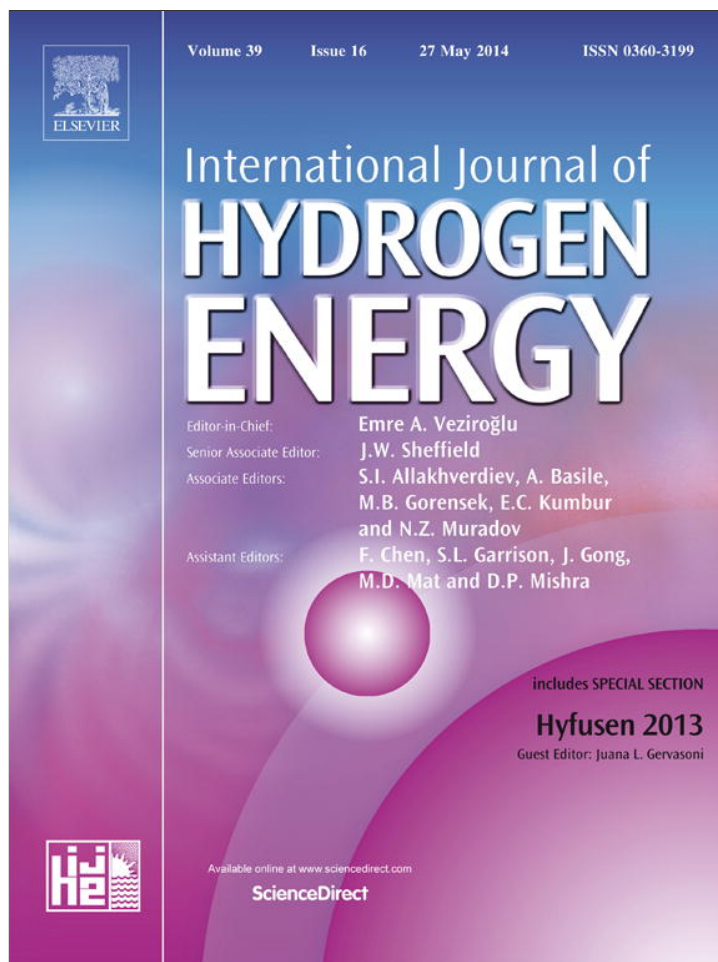


Provided for non-commercial research and education use.  
Not for reproduction, distribution or commercial use.



This article appeared in a journal published by Elsevier. The attached copy is furnished to the author for internal non-commercial research and education use, including for instruction at the authors institution and sharing with colleagues.

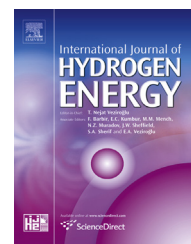
Other uses, including reproduction and distribution, or selling or licensing copies, or posting to personal, institutional or third party websites are prohibited.

In most cases authors are permitted to post their version of the article (e.g. in Word or Tex form) to their personal website or institutional repository. Authors requiring further information regarding Elsevier's archiving and manuscript policies are encouraged to visit:

<http://www.elsevier.com/authorsrights>

Available online at [www.sciencedirect.com](http://www.sciencedirect.com)

ScienceDirect

journal homepage: [www.elsevier.com/locate/he](http://www.elsevier.com/locate/he)

# Co catalysts modified by rare earths (La, Ce or Pr) for hydrogen production from ethanol

Mariana N. Barroso, Manuel F. Gomez, Luis A. Arrúa, M. Cristina Abello\*

Instituto de Investigaciones en Tecnología Química (UNSL-CONICET), Chacabuco y Pedernera, 5700 San Luis, Argentina

## ARTICLE INFO

### Article history:

Received 17 October 2013

Accepted 5 December 2013

Available online 4 January 2014

### Keywords:

Hydrogen production

Ethanol steam reforming

Co-catalysts

## ABSTRACT

Co/MgAl<sub>2</sub>O<sub>4</sub> catalysts modified with La, Pr or Ce were prepared, characterized by different techniques and tested in ethanol steam reforming reaction to produce hydrogen. The catalytic behavior at 650 °C depended on the nature of rare earth. The amount of carbon on promoted catalysts was significantly lower than that on unpromoted one. The Pr and La containing catalysts produced a high acetaldehyde selectivity which decreased the hydrogen production. The superior performance of the catalyst promoted with 7.8% Ce could be partially explained by a higher dispersion and a high reduction of Co species.

Copyright © 2013, Hydrogen Energy Publications, LLC. Published by Elsevier Ltd. All rights reserved.

## 1. Introduction

Nowadays the hydrogen is considered as the most attractive energy carrier since its combustion produces only water as product. However, its production in an efficient and economic way needs further research and development [1]. In the last years, hydrogen production from methane, methanol and ethanol reforming reactions has reached a great importance due to its application in fuel cells. It is particularly observed a great interest in catalysts development for hydrogen production from ethanol, a renewable resource with CO<sub>2</sub> formation reusable for the biomass. Several catalytic systems based on Ni and noble metals [2–6] have shown to be effective with different hydrogen selectivities. Co based catalysts have received less attention in the ethanol steam reforming in spite of their high capacity for C–C bond breaking similar to the Ni and noble metals. Different supports have been used for cobalt including Al<sub>2</sub>O<sub>3</sub>, ZnO, MgO, CeO<sub>2</sub>, ZrO<sub>2</sub>, etc. [7–15], these

catalysts have shown differences in activity, product distributions and resistance to coking and sintering. Recently, the activity of the Co catalysts was increased by adding of small amounts of noble metals [8,16]. The effects of the noble metals included a marked lowering of the reduction temperatures of the cobalt species interacting with the support and changes in the redox and electronic properties of Co sites. The promoted catalysts with Pt, Ru or Ir showed high selectivity to hydrogen without ethene formation. In previous works, Ni catalysts supported on MgAl<sub>2</sub>O<sub>4</sub> promoted with rare earths have shown a good catalytic performance in ethanol steam reforming [17,18] but also deactivation and pressure build-up under more practical reforming conditions.

In the current work, Co/MgAl<sub>2</sub>O<sub>4</sub> catalysts doped with La, Ce or Pr were prepared, characterized and tested in the ethanol steam reforming reaction for hydrogen production. Different characterization techniques were used to study the effect of rare earth nature on catalytic activity and on resistance to coking.

\* Corresponding author. Tel.: +54 266 4426711.

E-mail addresses: [mnbarro@unsl.edu.ar](mailto:mnbarro@unsl.edu.ar) (M.N. Barroso), [cabello@unsl.edu.ar](mailto:cabello@unsl.edu.ar) (M.C. Abello).

## 2. Experimental

### 2.1. Catalyst preparation

MgAl<sub>2</sub>O<sub>4</sub> support (MA) was prepared by the citrate method [18]. Citric acid was added to an aqueous solution that contained the stoichiometric quantities of Al(NO<sub>3</sub>)<sub>3</sub>·9H<sub>2</sub>O and Mg(NO<sub>3</sub>)<sub>2</sub>·6H<sub>2</sub>O. An equivalent of acid per total equivalent of metals was used. The solution was stirred for 10 min and held at boiling temperature for 30 min. Then, the solution was concentrated by evaporation under vacuum in a rotavapor at 75 °C until a viscous liquid was obtained. Finally, dehydration was completed by drying the sample in a vacuum oven at 100 °C for 16 h. The sample was calcined in static air from room temperature to 500 °C at a heating rate of 5° min<sup>-1</sup> and then at 700 °C for 2 h.

The addition of Co (8 wt.%) and rare earth (5 wt.%) into the support was sequentially carried out by wet impregnation using an aqueous solution of Co(CH<sub>3</sub>COO)<sub>2</sub>·4H<sub>2</sub>O, La(N-O<sub>3</sub>)<sub>3</sub>·6H<sub>2</sub>O, Ce(CH<sub>3</sub>COO)<sub>3</sub>·xH<sub>2</sub>O or Pr(CH<sub>3</sub>COO)<sub>3</sub>·xH<sub>2</sub>O. The solvent was removed in a rotating evaporator at 75 °C under vacuum. The samples were dried between the impregnation steps at 100 °C overnight. Finally, they were calcined in air at 600 °C for 3 h. The catalysts were denoted as Co/MAR being R: L, C or P indicative of lanthanum, cerium or praseodymium, respectively.

### 2.2. Catalyst characterization

All samples were characterized using different physico-chemical methods.

#### 2.2.1. Chemical composition

Lanthanum, cerium, praseodymium and cobalt chemical composition was performed by inductively coupled plasma-atomic emission spectroscopy (ICP) using a sequential ICP spectrometer Baird ICP 2070 (BEDFORD, USA) with a Czerny Turner monochromator (1 m optical path). Alkali fusion with KHSO<sub>4</sub> and a subsequent dissolution with HCl solution brought the samples into solution.

#### 2.2.2. BET surface area

BET surface areas were measured using a Micromeritics Gemini V analyzer by adsorption of nitrogen at -196 °C on 100 mg of a sample previously degassed at 250 °C for 16 h under flowing N<sub>2</sub>.

#### 2.2.3. X-ray diffraction (XRD)

Diffraction patterns were obtained with a RIGAKU diffractometer operated at 30 kV and 20 mA using Ni-filtered CuKα radiation (λ = 0.15418 nm) at a rate of 3° min<sup>-1</sup> from 2θ = 20°–80°. The powdered samples were analyzed without a previous treatment after deposition on a quartz sample holder. The identification of crystalline phases was made by matching with the JCPDS files.

#### 2.2.4. Thermal gravimetry (TG-TPO)

The analyses were recorded using DTG-60 Shimadzu equipment. The samples, ca. 15 mg, were placed in a Pt cell and

heated from room temperature to 1000 °C at a heating rate of 10 °C min<sup>-1</sup> with an air flow of 50 mL min<sup>-1</sup>. Carbon deposited during reaction on used catalysts was evaluated as

$$\%C = \frac{w_{\text{coke}}}{w_{\text{catalyst}}} \times 100$$

where  $w_{\text{coke}}$  is the coke mass deposited on the catalyst calculated from the weight loss measured by TGA and  $w_{\text{catalyst}}$  is the catalyst weight free of carbon remaining after the TG analysis.

#### 2.2.5. Temperature programmed reduction (TPR)

Studies were performed in a conventional TPR equipment. This apparatus consists of a gas handling system with mass flow controllers, a tubular reactor, a linear temperature programmer, a PC for data retrieval, a furnace and various cold traps. Before each run the samples were oxidized in a 50 mL min<sup>-1</sup> flow of 20 vol.% O<sub>2</sub> in He at 300 °C for 30 min. After that helium was admitted to remove oxygen and finally, the system was cooled to 25 °C. The samples were subsequently contacted with a 50 mL min<sup>-1</sup> flow of 5 vol.% H<sub>2</sub> in N<sub>2</sub>, heated at a rate of 10 °C min<sup>-1</sup> from 25 °C to a final temperature of 700 °C and held at 700 °C for 2 h. Hydrogen consumption was monitored by a thermal conductivity detector after removing the formed water. The peak areas were calibrated with H<sub>2</sub> (5 vol.%) / N<sub>2</sub> mixture injections.

#### 2.2.6. Scanning electron microscopy and energy dispersive X-ray spectroscopy (SEM-EDX)

Scanning electron micrographs were obtained in a LEO 1450 VP. This instrument equipped with an energy dispersive X-ray microanalyzer (EDAX Genesis 2000) and a Si(Li) detector allowed the analytical electron microscopy measurements. The samples were sputter coated with gold.

#### 2.2.7. Nitrous oxide chemisorption

Dispersion of cobalt was determined by the N<sub>2</sub>O chemisorption technique. Before each run the samples were oxidized in a 50 mL min<sup>-1</sup> flow of 20 vol.% O<sub>2</sub> in He at 300 °C for 30 min to eliminate possible surface contamination before the pre-reduction. After that helium was admitted to remove oxygen and finally, the system was cooled to 25 °C. The samples were subsequently contacted with a 30 mL min<sup>-1</sup> flow of 5 vol.% H<sub>2</sub> in N<sub>2</sub>, heated at a rate of 10 °C min<sup>-1</sup>, from 25 °C to a final temperature of 700 °C and held at 700 °C for 2 h. Then, the sample was flushed with He (30 mL min<sup>-1</sup>) at 700 °C for 30 min and cooled down to 40 °C. N<sub>2</sub>O chemisorption was carried out on the reduced catalyst by a N<sub>2</sub>O flow at 40 °C for 30 min [15]. The hydrogen consumptions, X for the first reduction and Y after surface oxidation by nitrous oxide chemisorption, were used to calculate cobalt metallic dispersion (D%), assuming the occurrence of the following reactions

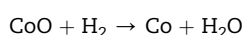
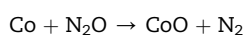
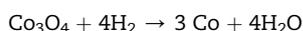


**Table 1 – Characteristics of fresh Co catalysts.**

Sample	Chemical composition, wt.%		S <sub>BET</sub> m <sup>2</sup> g <sup>-1</sup>	D <sup>b</sup> %
	Co	R <sup>a</sup>		
Co/MA	9.00	–	123	33.2
Co/MAL	6.35	4.35	102	32.2
Co/MAP	8.24	6.45	74	42.9
Co/MAC	6.50	7.81	73.6	45.2

<sup>a</sup> R: Rare earth (La, Ce or Pr). Nominal loading: 8.0 wt.% Co and 5.0 wt.% R.  
<sup>b</sup> Co dispersion over Co catalysts determined using N<sub>2</sub>O chemisorption.

$$D\% = (4Y/3X) \cdot 100$$

### 2.3. Catalytic test

The ethanol steam reforming reaction was carried out in a quartz tubular reactor with an internal diameter of 4 mm operated at atmospheric pressure and 650 °C. The reactor was placed in a vertical furnace with temperature control. The reaction temperature was measured with a coaxial K thermocouple placed inside the sample. The feed to the reactor was a gas mixture of ethanol, water and helium (99.999% research grade). The liquid mixture of ethanol–water was fed at 0.15 mL min<sup>-1</sup> to an evaporator (operated at 130 °C) through an isocratic pump. The gas stream flow rates were controlled by mass flowmeters. The experimental set-up has a low pressure proportional relief valve for early detection of catalytic bed plugging. The molar ratio in the feed was H<sub>2</sub>O: C<sub>2</sub>H<sub>5</sub>OH = 4.8 being the ethanol flow 1.02 × 10<sup>-3</sup> mol min<sup>-1</sup>.

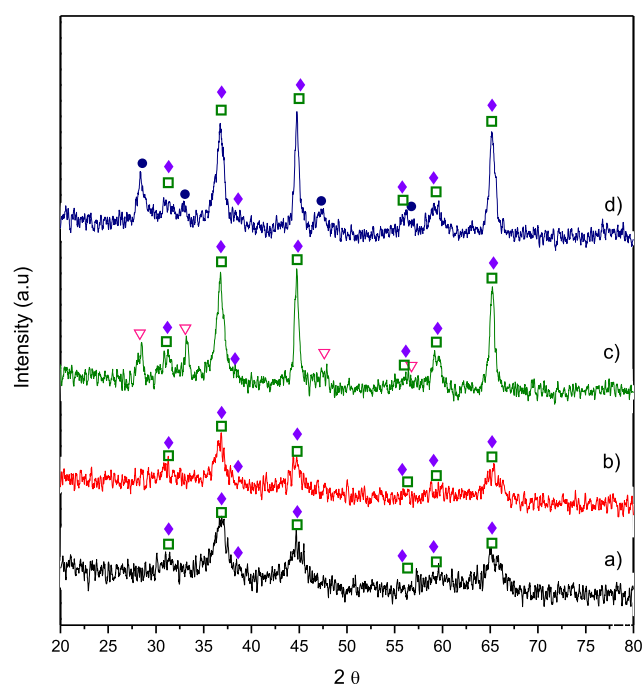


**Fig. 1 – X-ray diffraction patterns of fresh samples. (a) Co/MA, (b) Co/MAL, (c) Co/MAP and (d) Co/MAC. □: MgAl<sub>2</sub>O<sub>4</sub>, ◆: Co<sub>3</sub>O<sub>4</sub>, ▽: PrO<sub>2</sub>/Pr<sub>6</sub>O<sub>11</sub> □: CeO<sub>2</sub>.**

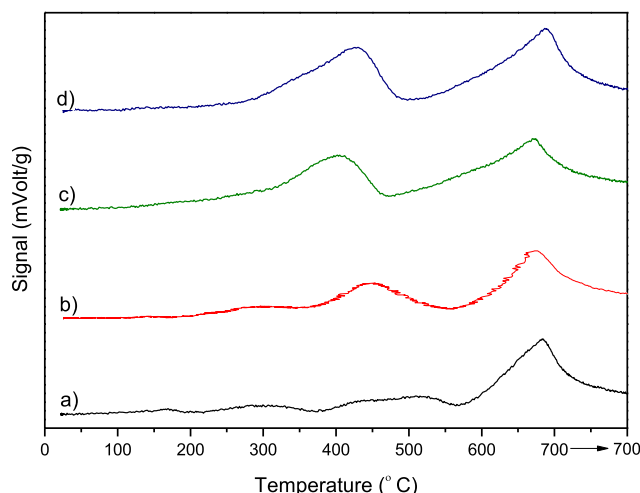


**Fig. 2 – Temperature programmed reduction profiles for (a) Co/MA, (b) Co/MAL, (c) Co/MAC and (d) Co/MAP.**

The molar ratio was near the optimum one suggested from a study of energy integration and maximum efficiency in an ethanol processor for hydrogen production and a fuel cell [19,20]. The catalyst weight was 50 mg (0.3–0.4 mm particle size range) without dilution in an inert material. Before reforming experiments, the catalyst was *in situ* reduced in H<sub>2</sub>(5%)/N<sub>2</sub> flow at 650 °C for 1 h. After a purge in He flow, the mixture with C<sub>2</sub>H<sub>5</sub>OH + H<sub>2</sub>O was allowed to enter into the reactor to carry out the catalytic test. The reactants and reaction products were analyzed on-line by gas chromatography. H<sub>2</sub>, CH<sub>4</sub>, CO<sub>2</sub> and H<sub>2</sub>O were separated by a 1.8 m Carbosphere (80–100 mesh) column and analyzed by TC detector. Nitrogen was used as an internal standard. Besides, CO was analyzed by a flame ionization detector after passing through a methanizer. Higher hydrocarbons and oxygenated products (C<sub>2</sub>H<sub>4</sub>O, C<sub>2</sub>H<sub>4</sub>+C<sub>2</sub>H<sub>6</sub>, C<sub>3</sub>H<sub>6</sub>O, C<sub>2</sub>H<sub>5</sub>OH, etc.) were separated in Rt-U PLOT capillary column and analyzed with FID using N<sub>2</sub> as carrier gas.

Ethanol conversion (X<sub>EtOH</sub>), selectivity to carbon products (S<sub>i</sub>) and hydrogen yield (Y<sub>H<sub>2</sub></sub>) were estimated as

$$X_{EtOH} = \frac{F_{EtOH}^{in} - F_{EtOH}^{out}}{F_{EtOH}^{in}} \times 100$$

$$S_i = \frac{\nu_i F_i^{out}}{2(F_{EtOH}^{in} - F_{EtOH}^{out})} \times 100$$

$$Y_{H_2} = \frac{F_{H_2}^{out}}{F_{EtOH}^{in}}$$

**Table 2 – TPR results for Co catalysts.**

Catalyst	T <sub>peak</sub> , °C		mol H <sub>2</sub> /mol Co
Co/MA	434–520	683	0.43
Co/MAL	448	674	0.54
Co/MAP	403	672	0.62
Co/MAC	428	687	0.61

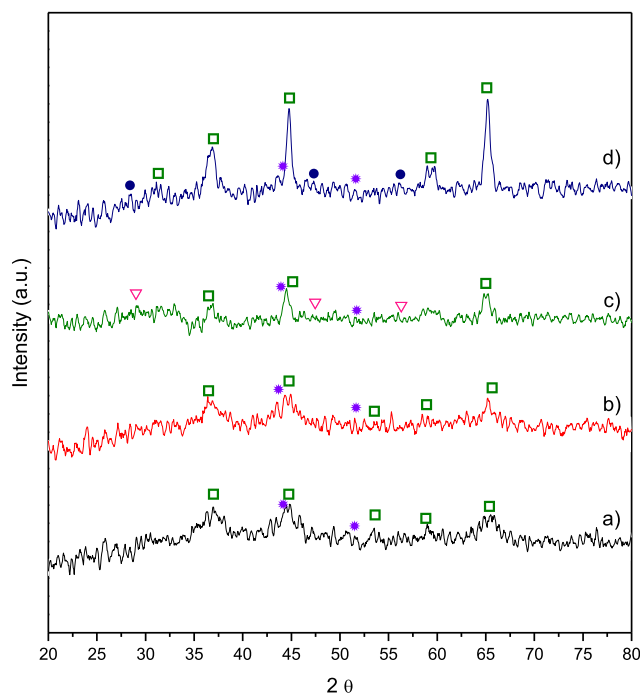


**Fig. 3 – X-ray diffraction patterns after TPR experiments. (a) Co/MA, (b) Co/MAL, (c) Co/MAP and (d) Co/MAC. □: MgAl<sub>2</sub>O<sub>4</sub>, \* : Co<sup>0</sup>, ▽: PrO<sub>2</sub>/Pr<sub>6</sub>O<sub>11</sub> ●: CeO<sub>2</sub>.**

$F_i^{\text{in}}$  and  $F_i^{\text{out}}$  are the molar flow rates of product “i” at the inlet and outlet of the reactor, respectively, and  $\nu_i$  is the number of carbon atoms in “i”.

### 3. Results and discussion

#### 3.1. Characterization of fresh catalysts

The chemical composition obtained by ICP and specific surface areas of catalysts after calcination are shown in Table 1. The Co composition is close to the nominal one. The  $S_{\text{BET}}$  are relatively high in spite of the thermal treatment at 600 °C for 3 h. The dopant addition decreases the  $S_{\text{BET}}$  being the lowest values for the catalysts modified with Ce or Pr, probably due to the plugging of the pores of aluminate with cerium and praseodymium oxides species. This is in a good agreement with the results reported in literature for the addition of CeO<sub>2</sub> to Al<sub>2</sub>O<sub>3</sub> and PrO<sub>2</sub> to Al<sub>2</sub>O<sub>3</sub> [21,22] although in our case the addition of lanthanide was carried out over the Co/MA sample.

The diffraction patterns of fresh samples, Fig. 1, present a small derivation in the baseline due to the typical fluorescence of Co containing materials. The peaks at  $2\theta = 31.3^\circ, 36.8^\circ, 44.8^\circ, 55.6^\circ, 59.4^\circ$  and  $65.2^\circ$  correspond to MgAl<sub>2</sub>O<sub>4</sub> (JCPDS-21-1152) and Co<sub>3</sub>O<sub>4</sub> (JCPDS-42-1467) since the reflexion lines are coincident. The surface presence of CoAl<sub>2</sub>O<sub>4</sub> (JCPDS-10-0458) cannot be ruled out but its formation should be negligible due to the previous thermal stabilization of the support. In literature it is reported that the calcination in air leads to Co<sub>3</sub>O<sub>4</sub> formation whereas the calcination in inert produces CoO [23]. Besides, the samples are dark green which is characteristic of Co<sup>3+</sup> ions in octahedral coordination [24]. Therefore, the cobalt should be mainly present in Co<sub>3</sub>O<sub>4</sub> form in fresh catalysts. In Co/MAP and Co/MAC samples, the reflexion lines of PrO<sub>2</sub>/Pr<sub>6</sub>O<sub>11</sub> and CeO<sub>2</sub> and an increase in crystallinity are observed. In Co/MAL sample La-compounds are not detected and its diffraction pattern resembles to that Co/MA.

Profiles of temperature programmed reduction with H<sub>2</sub> (TPR) are shown in Fig. 2. For the Co/MA sample the profile shows an intense peak at high temperature and two small ones at lower temperatures. They can be assigned to different Co<sup>3+</sup>/Co<sup>2+</sup> species. Similar results are observed for Co/MAL catalyst, in agreement with XRD patterns. The presence of La in Co/MA catalyst has little effect on the reduction temperature of Co species in contrast to the addition of Pr or Ce. The reduction profiles for Co/MAC and Co/MAP show two intense peaks at 428° and 687 °C and 403° and 672 °C, respectively. The peak at low temperature could be attributed to the reduction of Co<sup>3+</sup>/Co<sup>2+</sup> (Co<sub>3</sub>O<sub>4</sub>) and the peak at the highest temperature, between 600 and 700 °C, could be associated to the reduction of Co species strongly interacted with the MgAl<sub>2</sub>O<sub>4</sub>. A summary of TPR results is shown in Table 2. The reduction extent measured as mol H<sub>2</sub>/mol Co clearly indicates that the cobalt species are not completely reduced at 650 °C. These results suggest that different Co species (Co<sup>0</sup> and Co<sup>δ+</sup>) could be present on the catalytic surface at the beginning of reaction. The surface reduction of cerium and praseodymium oxides also contribute to the observed hydrogen consumption. The peak at the high temperature (>600 °C) is similar in the four samples whereas the first peak shifts to a lower temperature, suggesting that the lanthanide presence favors the Co reducibility and decreases the interaction of these species with the aluminate matrix, specially with the addition of Ce and Pr. Similar results have been reported by Lucredio et al. [25] for Co catalysts derived from hydrotalcite (Co/Mg/Al) modified with La and Ce.

The XRD patterns of reduced samples, Fig. 3, reveal low intensity peaks (the amount of sample used to collect the diffraction pattern was small) which could be assigned to MgAl<sub>2</sub>O<sub>4</sub>. Cerium and praseodymium oxides are also detected

**Table 3 – Catalytic results in ethanol steam reforming reaction over Co catalysts.**

Catalyst	$X_{\text{EtOH}}\%$	$S_{\text{CO}_2}\%$	$S_{\text{CO}}\%$	CO/CO <sub>2</sub>	$S_{\text{CH}_3\text{CHO}}\%$	$S_{\text{CH}_4}\%$	mol H <sub>2</sub> /mol EtOH
Co/MA	87(0.71)	30	32	1.07	25	5	3.4
Co/MAL	76(0.74)	22	21	0.95	46	6	2.4
Co/MAP	85(1.15)	28	34	1.21	21	4	2.8
Co/MAC	100(1.36)	47	39	0.83	3	6	5.2

The values of conversion and selectivity correspond at 420 min on stream. The values between brackets correspond to specific conversions ( $X\%/S_{\text{BET}}$ ).

in Co/MAP and Co/MAC samples. Peaks corresponding to  $\text{Co}^0$  ( $2\theta = 44.3^\circ, 51.4^\circ, 75.8^\circ$ , JCPDS-15-0806) are almost undetected suggesting that Co particles are highly dispersed on aluminate matrix. Peaks related to lanthanum oxides are not observed.

Co dispersions over the reduced samples were determined by  $\text{N}_2\text{O}$  chemisorption experiments. The dispersion data, D%,

**Table 4 – Carbon amount determined by TG-TPO.**

Catalyst	%C	$\frac{\text{mol C}_{\text{deposited}}}{\text{mol C}_{\text{inlet}}} \cdot 10^3$	$T_{\text{burning}}, ^\circ\text{C}$
Co/MA	30.2	1.286	521
Co/MAL	22.6	1.097	544
Co/MAP	22.5	1.095	495
Co/MAC	22.9	0.994	496

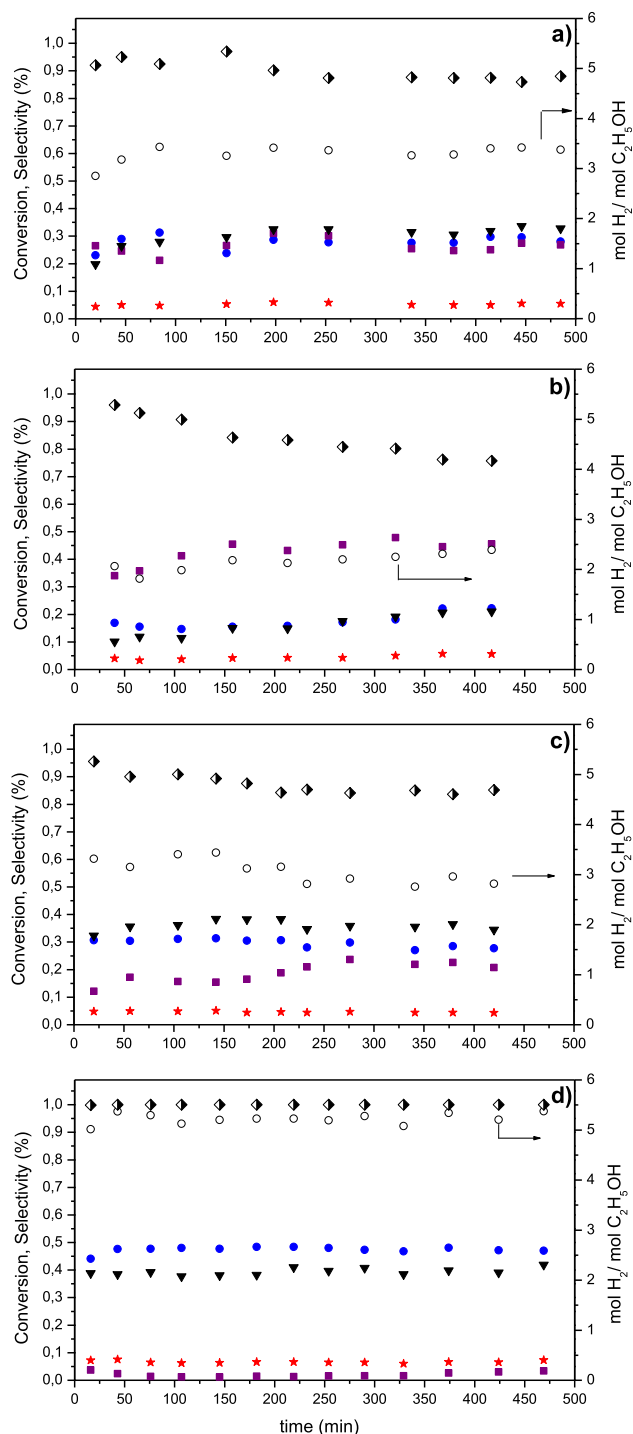


**Fig. 4 – Conversion and product distribution in the ethanol steam reforming reaction over (a) Co/MA, (b) Co/MAL, (c) Co/MAC and (d) Co/MAP at 650 °C and atmospheric pressure.  $\blacklozenge$  ethanol conversion;  $\circ$ : mol  $\text{H}_2$ /mol  $\text{C}_2\text{H}_5\text{OH}$ ;  $\blacksquare$ :  $\text{C}_2\text{H}_4\text{O}$ ;  $\star$ :  $\text{CH}_4$ ;  $\bullet$ :  $\text{CO}_2$ ;  $\blacktriangledown$ :  $\text{CO}$ .**

shown in Table 1, follows the order of  $\text{Co/MAC} > \text{Co/MAP} > \text{Co/MA} \approx \text{Co/MAL}$ . The Ce containing catalyst with the highest dispersion leads to the highest  $\text{H}_2$  production and the La containing catalyst with the lowest dispersion leads to the lowest  $\text{H}_2$  production (see further). The importance of Co dispersion for the hydrogen production was also reported in Co/CeO<sub>2</sub> catalysts prepared from different cobalt precursors [15]. However, the  $\text{H}_2$  yields for the other two catalysts did not show a clear trend with dispersion.

### 3.2. Catalytic behavior in the ethanol steam reforming

The catalytic activity of four samples is studied in the ethanol steam reforming reaction at 650 °C with a previous reduction in hydrogen. All the samples are active with high ethanol conversion at the beginning of the reaction despite the small amount of catalyst (50 mg). The catalyst with La (Co/MAL) shows a loss in activity after 420 min in time on stream (21%). Table 3 summarizes the conversion and the product distribution at the end of the experiment (420 min). The specific conversion ( $X/S_{\text{BET}}$ ) follows the order of  $\text{Co/MAC} > \text{Co/MAP} > \text{Co/MAL} \approx \text{Co/MA}$ .

The addition of lanthanide improves the initial ethanol conversion but the product distributions illustrated in Fig. 4 show differences in the reaction pathway proposed for the ethanol steam reforming. In all the cases the main reaction products are  $\text{H}_2$ ,  $\text{CO}_2$ ,  $\text{CO}$ ,  $\text{CH}_4$  and  $\text{CH}_3\text{CHO}$  at 650 °C. In Table 3 the selectivity to  $\text{CH}_3\text{CHO}$ , the molar ratio  $\text{CO}/\text{CO}_2$  and  $\text{H}_2$  yield expressed as  $\text{mol H}_2/\text{mol C}_2\text{H}_5\text{OH}$  are compared. The hydrogen yield follows the order of  $\text{Co/MAC} \gg \text{Co/MA} > \text{Co/MAP} > \text{Co/MAL}$ . The Ce-containing catalyst with the highest Co dispersion leads to the highest production of hydrogen and the lowest acetaldehyde selectivity (3%). Similar results were found on CeNi catalysts [26]. The selectivity to  $\text{CH}_3\text{CHO}$  on La-containing catalyst is the highest among the tested catalysts (46%) indicating a loss in the reforming capacity. This loss in the breaking capacity of C–C bond with the addition of La could be a consequence of a higher fraction of  $\text{Co}^{\delta+}$  during reaction.  $\text{Co}_3\text{O}_4$  has been reported to be the active phase for ethanol dehydrogenation and  $\text{Co}^0$  for acetaldehyde reforming [27,28]. In fact when these Co/MAR catalysts were tested without a previous reduction the main reaction product was acetaldehyde. The formation of  $\text{CH}_3\text{CHO}$  is also high on Co/MA (25%) and Co/MAP (21%). As regards the aldehyde selectivity the same behavior was found over Ni supported on  $\text{MgAl}_2\text{O}_4$  modified with Ce or Pr when they were tested in the same reforming conditions. At the steady state, the selectivities to acetaldehyde were lower in the Ce doped catalyst ( $S_{\text{CH}_3\text{CHO}} = 2.9\%$ ) than in the Pr doped sample ( $S_{\text{CH}_3\text{CHO}} = 9.5\%$ ) [18]. The  $\text{CH}_4$  formation is similar in all the samples with selectivities between 4 and 6% and it is almost not affected by

the lanthanide nature. Ethylene is not observed in any case probably because the support used is basic [8,29].

The product distribution for the catalyst modified with Ce (Co/MAC) is the most stable with reaction time. No signal of deactivation is observed during 420 min on stream though the carbon balance during this period suggests coking deposition. This was verified by post-characterization of the catalyst. Although the catalytic behavior and  $H_2$  yield over this system is quite promising, stability tests at long time on stream

should be carried out, particularly if it is taken into account that it produces carbonaceous species in the form of filaments (as shown further).

### 3.3. Characterization of used catalysts

TG results under oxygen flow shown in Table 4 reveal a significant decrease in the %C (around 25%) on the modified catalysts and also a significant decrease in the burning

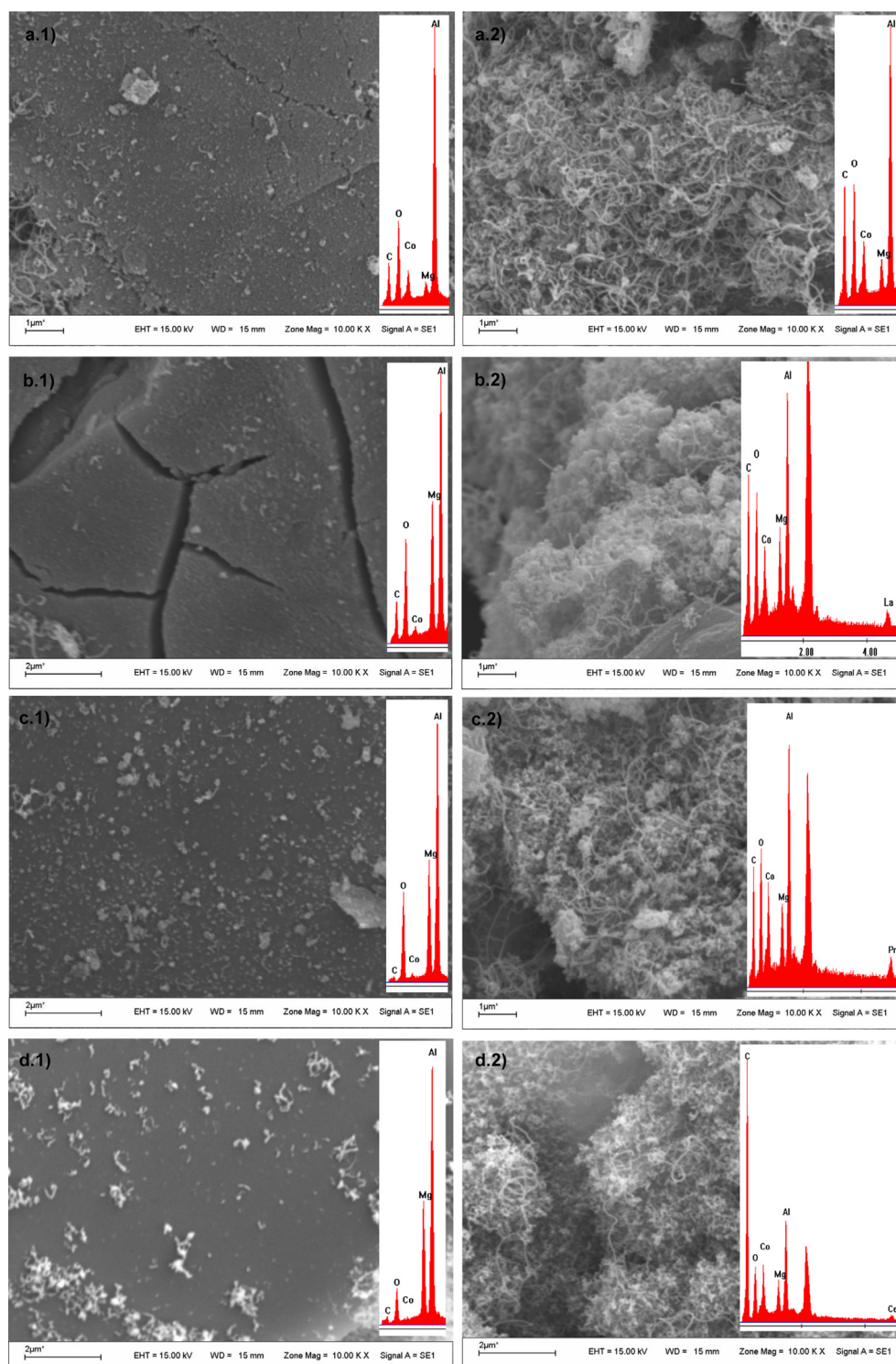


Fig. 5 – SEM images of used (a) Co/MA, (b) Co/MAL, (c) Co/MAP and (d) Co/MAC catalysts.

temperature on those with Ce or Pr. The burning temperature is high, suggesting a high extent of carbon deposit graphitization [6]. Bearing in mind that the %C is similar for catalysts modified with lanthanide, the lower burning temperature could be indicating differences in the fiber structure (parallel or fishbone type). Ros et al. have reported that the maximum oxidation rate for parallel fiber occurs at lower temperature [30]. The parallel fibers are characterized for a center hole and the metallic particle on the tip. The average carbon deposition rate expressed as mol of C deposited per mol of C in the feed follows the order of Co/MAC < Co/MAP  $\approx$  Co/MAL < Co/MA. These carbon deposition rates are similar to others on Ni/Mg/Al catalysts with Ce or La [27].

The SEM micrographs of the used catalysts are shown in Fig. 5. Two different regions are observed: (i) a zone that is almost free of carbonaceous deposits and also of lanthanide with a low Co concentration; (ii) a zone with an abundant filament formation where Co and lanthanide signals are detected by EDX. This behavior is suggesting that the metallic Co is exposed at the tip of a fiber (justifying the negligible deactivation observed during 420 min on stream) and that the lanthanide is interacting with a fraction of Co particles more than with MgAl<sub>2</sub>O<sub>4</sub>, likely due to the sequence of impregnation. From TPR the extent of Co interaction with the support decreases with lanthanide addition. The lanthanide oxides would interact in a different way with the Co particles, particularly CeO<sub>2</sub> and PrO<sub>x</sub>.

The influence of redox properties of Ce and Pr have been studied in ethanol steam reforming over Ni/MgAl<sub>2</sub>O<sub>4</sub> catalysts. By XPS these Ce-promoted solids presented the Ce<sup>3+</sup>/Ce<sup>4+</sup> couple on the surface even after treatment in a reductive atmosphere. On the contrary, Pr-doped catalysts showed a very high concentration of Pr<sup>3+</sup> [31]. Similar behavior would be found over Co catalysts. The question to how the La-containing catalyst leads to a lower catalytic performance in ethanol reforming remains unclear and will require further characterization.

#### 4. Conclusions

Co/MgAl<sub>2</sub>O<sub>4</sub> catalysts modified by the addition of Ce, Pr or La were active in the ethanol steam reforming reaction, with initial ethanol conversions higher than 80% at 650 °C and 50 mg of catalyst. No significant deactivation was observed during 420 min on stream although carbonaceous deposits were determined by TG-TPO experiments and by SEM examination. The amount of carbon on promoted catalysts was significantly lower than that on unpromoted one. The Pr and La containing catalysts produced a high acetaldehyde selectivity which decreased the hydrogen production. The superior performance of the catalyst promoted with 7.8% Ce could be partially explained by a higher dispersion and a high reduction of Co species.

#### Acknowledgments

Financial supports are acknowledged to CONICET, ANPCyT and Universidad Nacional de San Luis. The authors are

grateful to Lic. Esther Fixman by the chemisorption measurements.

#### REFERENCES

- [1] Song H, Ozkan US. Economic analysis of hydrogen production through a bio-ethanol steam reforming process: sensitivity analyses and cost estimations. *Int J Hydrogen Energy* 2010;35:127–34.
- [2] Ni M, Leung DY, Leung MK. A review on reforming bioethanol for hydrogen production. *Int J Hydrogen Energy* 2007;32:3238–47.
- [3] Vaidya PD, Rodrigues AE. Insight into steam reforming of ethanol to produce hydrogen for fuel cells. *Chem Eng J* 2006;117:39–49.
- [4] Dal Santo V, Gallo A, Naldoni A, Guidotti M, Psaro R. Bimetallic heterogeneous catalysts for hydrogen production. *Catal Today* 2012;197:190–205.
- [5] Galetti AE, Gomez MF, Arrúa LA, Abello MC. Ni catalysts supported on modified ZnAl<sub>2</sub>O<sub>4</sub> for ethanol steam reforming. *App Catal A Gen* 2010;380:40–7.
- [6] Sanchez-Sanchez MC, Navarro RM, Fierro JLG. Ethanol steam reforming over Ni/M<sub>x</sub>O<sub>y</sub>-Al<sub>2</sub>O<sub>3</sub> (M = Ce, La, Zr and Mg) catalysts: influence of support on the hydrogen production. *Int J Hydrogen Energy* 2007;32:1462–71.
- [7] Llorca J, Homs N, Sales J, Ramirez de la Piscina P. Efficient production of hydrogen over supported cobalt catalysts from ethanol steam reforming. *J Catal* 2002;209:306–17.
- [8] Profeti LPR, Ticianelli EA, Assaf EM. Production of hydrogen by ethanol steam reforming on Co/Al<sub>2</sub>O<sub>3</sub> catalysts: effect of addition of small quantities of noble metals. *J Power Sources* 2008;175:482–9.
- [9] Batista M, Santos R, Assaf E, Assaf J, Ticianelli E. Characterization of the activity and stability of supported cobalt catalysts for the steam reforming of ethanol. *J Power Sources* 2003;124:99–103.
- [10] Llorca J, Homs N, Sales J, Fierro JLG, Ramirez de la Piscina P. Effect of sodium addition on the performance of Co-ZnO-based catalysts for hydrogen production from bioethanol. *J Catal* 2004;222:470–80.
- [11] Sahoo DR, Vajpai S, Patel S, Pant KK. Kinetic modeling of steam reforming of ethanol for the production of hydrogen over Co/Al<sub>2</sub>O<sub>3</sub> catalyst. *Chem Eng J* 2007;125:139–47.
- [12] Song H, Zhang L, Ozkan U. Effect of synthesis parameters on the catalytic activity of Co-ZrO<sub>2</sub> for bio-ethanol steam reforming. *Green Chem* 2007;9:686–94.
- [13] Lin S, Kim DH, Ha SY. Metallic phases of cobalt-based catalysts in ethanol steam reforming: the effect of cerium oxide. *App Catal A Gen* 2009;355:69–77.
- [14] Song H, Ozkan US. Ethanol steam reforming over Co-based catalysts: role of oxygen mobility. *J Catal* 2009;261:66–74.
- [15] Song H, Mirkelamoglu B, Ozkan US. Effect of cobalt precursor on the performance of ceria-supported cobalt catalysts for ethanol steam reforming. *App Catal A Gen* 2010;382:58–64.
- [16] Profeti LPR, Ticianelli EA, Assaf EM. Ethanol steam reforming for production of hydrogen on magnesium aluminate-supported cobalt catalysts promoted by noble metals. *App Catal A Gen* 2009;360:17–25.
- [17] Barroso MN, Galetti AE, Abello MC. Ni catalysts supported over MgAl<sub>2</sub>O<sub>4</sub> modified with Pr for hydrogen production from ethanol steam reforming. *App Catal A Gen* 2011;394:124–31.
- [18] Galetti AE, Barroso MN, Gomez MF, Arrua LA, Monzón A, Abello MC. Promotion of Ni/MgAl<sub>2</sub>O<sub>4</sub> catalysts with rare earths for the ethanol steam reforming reaction. *Catal Letters* 2012;142:1461–9.

- [19] Francesconi JA, Mussati MC, Mato RO, Aguirre PA. Analysis of the energy efficiency of an integrated ethanol processor for PEM fuel cell systems. *J Power Sources* 2007;167:151–61.
- [20] Perna A. Hydrogen from ethanol: theoretical optimization of a PEMFC system integrated with a steam reforming processor. *Int J Hydrogen Energy* 2007;32:1811–9.
- [21] Damyanova S, Perez CA, Schmal M, Bueno JMC. Characterization of ceria-coated alumina carrier. *App Catal A Gen* 2002;234:271–82.
- [22] Tankov I, Pawelec B, Arishtirova K, Damyanova S. Structure and surface properties of praseodymium modified alumina. *Appl Surf Sci* 2011;258:278–84.
- [23] Marchi AJ, Di Cosimo JI, Apesteguía CR. Effect of the preparation conditions on the reducibility of Cu-Co based oxides. *Catal Today* 1992;15:383–94.
- [24] Arnoldy P, Moulijn JA. Temperature-programmed reduction of  $\text{CoOAl}_2\text{O}_3$  catalysts. *J Catal* 1985;93:38–54.
- [25] Lucrecio AF, Bellido JA, Assaf EM. Cobalt catalysts derived from hydrotalcite-type precursors applied to steam reforming of ethanol. *Catal Comm* 2011;12:1286–90.
- [26] Lucrecio AF, Bellido JDA, Assaf EM. Effects of adding La and Ce to hydrotalcite-type Ni/Mg/Al catalyst precursors on ethanol steam reforming reactions. *App Catal A Gen* 2010;388:77–85.
- [27] Llorca J, Homs N, Ramirez de la Piscina P. In situ DRIFT-mass spectrometry study of the ethanol steam-reforming reaction over carbonyl-derived Co/ZnO catalysts. *J Catal* 2004;227:556–60.
- [28] Casanovas A, Roig M, de Leitenburg C, Trovarelli A, Llorca J. Ethanol steam reforming and water gas shift over Co/ZnO catalytic honeycombs doped with Fe, Ni, Cu, Cr and Na. *Int J Hydrogen Energy* 2010;35:7690–8.
- [29] Barroso MN, Galetti AE, Gomez MF, Arrúa LA, Abello MC. Ni-catalysts supported on  $\text{Zn}_x\text{Mg}_{1-x}\text{Al}_2\text{O}_4$  for ethanol steam reforming: influence of the substitution for Mg on catalytic activity and stability. *Chem Eng J* 2013;222:142–9.
- [30] Ros T, Van Dillen A, Geus J, Koningsberger D. Surface oxidation of carbon nanofibres. *Chem Eur J* 2002;8:1151–61.
- [31] Tarditi AM, Barroso MN, Galetti AE, Gómez MF, Arrúa LA, Cornaglia L, et al. Catalizadores de Ni soportados en  $\text{MgAl}_2\text{O}_4$  modificados con tierras raras (Pr o Ce) para la producción de hidrógeno. In: Caracterización por XPS. Acta XXIII Congreso Iberoamericano de Catálisis. Argentina: Santa Fe 2012.